THE JOURNAL OF PHYSICAL CHEMISTRY A

Article

pubs.acs.org/JPCA

Thermal Decomposition of 3-Bromopropene. A Theoretical Kinetic Investigation

María E. Tucceri,* María P. Badenes, Larisa L. B. Bracco, and Carlos J. Cobos

Instituto de Investigaciones Fisicoquímicas Teóricas y Aplicadas (INIFTA), Departamento de Química, Facultad de Ciencias Exactas, Universidad Nacional de La Plata, CONICET, Casilla de Correo 16, Sucursal 4, La Plata 1900, Argentina

Supporting Information

ABSTRACT: A detailed kinetic study of the gas-phase thermal decomposition of 3-bromopropene over wide temperature and pressure ranges was performed. Quantum chemical calculations employing the density functional theory methods B3LYP, BMK, and M06-2X and the CBS-QB3 and G4 ab initio composite models provide the relevant part of the potential energy surfaces and the molecular properties of the species involved in the $CH_2{=}CH{-}CH_2Br \rightarrow CH_2{=}C{=}CH_2 + HBr$ (1) and $CH_2{=}CH{-}CH_2Br \rightarrow CH_2{=}CH{-}CH_2 + Br$ (2) reaction channels. Transition-state theory and unimolecular reaction rate theory calculations show that the simple bond fission reaction (2) is the predominant decomposition channel and that all reported experimental studies are very close to the high-pressure limit of this process. Over the 500−1400 K range a rate constant for the primary dissociation of $k_{2,\infty} = 4.8 \times 10^{14}$ exp(−55.0 kcal mol^{-1}/RT) s^{-1} is predicted at the G4 level. The calculated $k_{1,\infty}$ values lie between 50 to 260 times smaller. A value of 10.6 ± 1.5 kcal mol^{-1} for the standard enthalpy of formation of 3-bromopropene at 298 K was estimated from G4 thermochemical calculations.

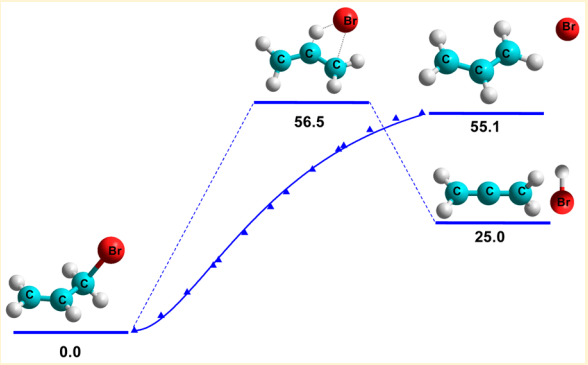

1. INTRODUCTION

Numerous applications ranging from industrial chemistry to laboratory synthesis are reported in the extensive literature on the chemistry of bromine compounds. In addition, it is known that some bromine species are active in the atmosphere.[1] To evaluate the environmental impact of these compounds the knowledge of their abundances, profiles, and reaction mechanisms is required. For these reasons a number of investigations including field campaigns, experimental and theoretical studies, and atmospheric modeling have been motivated.[2−4]

Here, we present the first detailed theoretical kinetic study on the thermal decomposition of 3-bromopropene. This species is an alkylating agent used in synthesis of polymers, pharmaceuticals, allyls, and other organic compounds. The present work was stimulated by investigations reported in the literature, which provide contradictory and incomplete kinetic information on this reaction. There are three main processes by which the thermal decomposition of 3-bromopropene may occur: the 2,3-elimination of HBr (1), the breaking of the C−Br bond (2), and the 3,3-elimination of HBr conducing to the $CH_2{=}CH{-}CH$ biradical (3).

$$CH_2{=}CH{-}CH_2Br \rightarrow CH_2{=}C{=}CH_2 + HBr \quad (1)$$

$$CH_2{=}CH{-}CH_2Br \rightarrow CH_2{=}CH{-}CH_2 + Br \quad (2)$$

$$CH_2{=}CH{-}CH_2Br \rightarrow CH_2{=}CH{-}CH + HBr \quad (3)$$

Maccoll studied the kinetics of the 3-bromopropene pyrolysis in a static system at above 300 Torr total pressure.[5] He proposed that the reaction takes place by the initial step (2), with a rate constant represented by the Arrhenius expression $k = 2.11 \times 10^{12}$ exp(−45.5 kcal mol^{-1}/RT) s^{-1} between 593 and 653 K. Besides, Szwarc et al. investigated the same reaction in a stream of toluene over the 732−865 K temperature range and pressures of 6−18 Torr.[6] They also concluded that the reaction evolves via process (2) with an activation energy of 47.5 ± 2 kcal mol^{-1} and a preexponential factor of 5×10^{12} s^{-1}. Moreover, Benson and O'Neal considered these results unreliable, and, on thermodynamic grounds, they recommended the rate expression $k = 2.0 \times 10^{14}$ exp(−56.4 kcal mol^{-1}/RT) s^{-1} for reaction (2).[7] They have also suggested that the reaction follows a chain decomposition mechanism. More recently, Tsang studied the 3-bromopropene unimolecular decomposition by a single-pulse shock-tube technique over the range of 830−1000 K in the presence of cyclopentane and at Ar total pressures ranging from 1444 to 3572 Torr.[8] In these experiments, the absence of allene as a product provided conclusive evidence that dehydrobromination (1) does not occur. The determined rate constants for reaction (2) at 1444 and 3572 Torr were, respectively, 2.5×10^{14} exp(−52.8 kcal

Received: December 23, 2015
Revised: March 17, 2016
Published: March 29, 2016

DOI: 10.1021/acs.jpca.5b12581
J. Phys. Chem. A 2016, 120, 2285−2294

mol^{-1}/RT) s^{-1} and 4.0 × 10^{14} exp(−53.5 kcal mol^{-1}/RT) s^{-1}, while at the high-pressure limit a rate constant of k_∞ = 1.0 × 10^{15}exp(−54.7 kcal mol^{-1}/RT) s^{-1} was obtained. On the other hand, Kim et al. studied the pyrolysis in a static system in the presence of butane as radical inhibitor over the 613−653 K and 4−170 Torr ranges.[9] Under these conditions, only process (1) was assumed important, being the derived activation energy of 50.04 kcal mol^{-1} and the preexponential factor of 2.6 × 10^{13} s^{-1}. More recently, Nisar and Awan investigated the pyrolysis of pure 3-bromopropene in a static Pyrex reaction vessel at 568.2−653.2 K and 14−64 Torr.[10] They analyzed the two possible primary processes (1) and (2), and the only products observed were allene and 1,5-hexadiene. All global kinetic data were well-represented by the expression k = 2.96 × 10^9 exp(−36.73 ± 1.6 kcal mol^{-1}/RT) s^{-1}. The experimental evidence led the authors to conclude that channel (2) is the predominant reaction pathway.

Because of the large uncertainties observed in the kinetic data reported for 2-chloropropene and 2-bromopropene decomposition reactions, quantum chemical and theoretical kinetic studies have been recently performed to elucidate these discrepancies.[11,12] To clarify the above-mentioned differences, the unimolecular reaction rate theory combined with potential energy surfaces derived via reliable quantum mechanical calculations were employed in the present study. An analysis of the energetics of the reaction channels (1)−(3), and the prediction of the rate constants over wide ranges of temperatures and pressures, are included in this investigation. The results presented here allow a comparison among all available experimental rate constants and predict the dominant reaction channel for determined temperature and pressure conditions.

2. COMPUTATIONAL METHODS

All the calculations were performed with the Gaussian09 program package.[13] The B3LYP,[14−16] BMK,[17] and M06-2X[18] formulations of the density functional theory (DFT) combined with the Pople triple split-valence basis set 6-311++G(3df,3pd) were employed. In addition, energy estimates were performed by using the high-level ab initio composite methods CBS-QB3[19,20] and G4.[21] In all cases, the structural parameters were fully optimized via analytic gradient methods. Harmonic vibration frequencies were computed employing analytical second-order derivative methods. The Synchronous Transit-Guided Quasi-Newton (STQN) method was employed for locating transition structures. The transition state was verified by following the intrinsic reaction coordinate (IRC) to both reactants and products at the M06-2X/6-311++G(3df,3pd) level of theory.

3. RESULTS AND DISCUSSION

3.1. Molecular Parameters and Harmonic Vibrational Frequencies. The structural parameters and harmonic vibrational frequencies for the 3-bromopropene and the species involved in reactions (1)−(3) were obtained using the aforementioned quantum-chemical models. Particularly, the frequencies derived at the CBS-QB3 and G4 levels were scaled by factors of 0.918 44[19,20] and 0.9854,[21] respectively. The results are shown in Figure 1 and Tables 1, 2, and S1 (in the Supporting Information). The obtained bond lengths, bond angles, and vibrational frequencies for 3-bromopropene at the employed levels differ in only ±0.04 Å, ±1.1°, and ±18 cm^{-1}, respectively. A very good agreement between these and reported experimental[22−24] and calculated[25] values was also found.

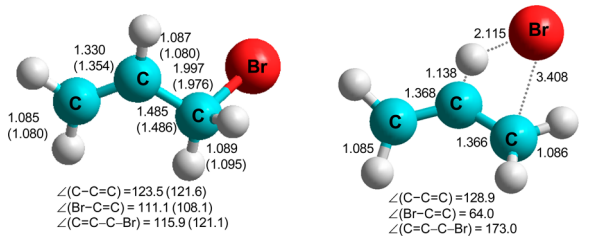

Figure 1. Geometrical structures of 3-bromopropene and the transition state for channel (1) obtained at the G4 level of theory. Bond distances in angstroms, angles in degrees. Experimental values from ref 22 are given between parentheses.

3.2. Thermochemistry and Energetics. To estimate the enthalpy changes for reactions (1)−(3), the standard enthalpy of formation for 3-bromopropene was determined employing the following isodesmic and isogyric reactions.

$$CH_2{=}CHBr + CH_3{-}CH_3 \rightarrow CH_2{=}CH{-}CH_2Br + CH_4 \quad (4)$$

$$CH_3{-}CH_2Br + CH_2{=}CH_2 \rightarrow CH_2{=}CH{-}CH_2Br + CH_4 \quad (5)$$

$$CH_3Br + CH_3{-}CH_3 + CH_2{=}CH_2 \rightarrow CH_2{=}CH{-}CH_2Br + 2CH_4 \quad (6)$$

In these hypothetic working reactions the number of each type of bonds in reactants and products and the spin multiplicities are conserved.[26] To derive the enthalpies of formation at 298 K, $\Delta H_{f,298}$, the recommended values from Active Thermochemical Database[27] (in kcal mol^{-1}) for CH_2CHBr (17.61 ± 0.15), CH_3CH_3 (−20.02 ± 0.04), CH_4 (−17.814 ± 0.014), CH_3CH_2Br (−15.09 ± 0.07), CH_2CH_2 (12.56 ± 0.04), and CH_3Br (−8.70 ± 0.05) were used. The resulting average $\Delta H_{f,298}$ values for 3-bromopropene are 11.2 (M06-2X), 8.9 (CBS-QB3), and 10.6 kcal mol^{-1} (G4). Besides enthalpies of formation of 14.5 (M06-2X), 7.4 (CBS-QB3), and 10.7 (G4) kcal mol^{-1} were derived from total atomization energies, based on atomic experimental enthalpies and estimated thermal contributions from refs 28 and 29. Our results at the G4 level are in very good agreement with the experimental values of Trager[30] of 11.4 kcal mol^{-1} and of 10.9 ± 1.6 kcal mol^{-1} derived by Cox and Pilcher[31] from data of ref 32, both reported in the NIST evaluation.[33] Therefore, we recommend the $\Delta H_{f,298}$ value obtained at the G4 level of 10.6 ± 1.5 kcal mol^{-1}. The stated conservative error limits are based on the experimental enthalpies errors and the dispersion of the obtained values.

Table 3 shows the enthalpies of reactions (1)−(3) estimated using the $\Delta H_{f,298}$ values derived here, together with those calculated directly from individual enthalpies obtained by adding to the total electronic energy, the zero-point energies, the RT term, and the contributions of the vibrational, rotational, and translational energies at different levels of theory. Enthalpy of formation values of −8.56 ± 0.04, 26.733 ± 0.013, 45.45 ± 0.09, and 39.70 ± 1.03 kcal mol^{-1} were used for HBr, Br, CH_2CCH_2, and CH_2CHCH_2, respectively.[27,34] As can

DOI: 10.1021/acs.jpca.5b12581
J. Phys. Chem. A 2016, 120, 2285−2294

Table 1. Harmonic Vibrational Frequencies (in cm^{-1}), Approximate Assignments, Rotational Constants (in cm^{-1}), and Torsional Barrier (in kcal mol^{-1}) for 3-Bromopropene Calculated at Different Levels of Theory

	3-bromopropene					
parameters	BMK	M06-2X	B3LYP	CBS-QB3	G4	exp[a]
vibrational frequencies						
stretching asym. $C(1)H_2$	3245	3238	3224	2957	3188	3100
stretching asym. $C(3)H_2$	3190	3182	3170	2911	3131	3032
stretching asym. C(2)H	3174	3166	3153	2893	3115	3018
stretching sym. $C(1)H_2$	3150	3145	3137	2877	3102	2995
stretching sym. $C(3)H_2$	3115	3108	3099	2845	3056	2977
stretching C=C	1707	1734	1696	1560	1682	1643
bending $C(3)H_2$	1511	1488	1488	1365	1461	1443
bending CH_2	1466	1449	1451	1328	1425	1416
bending HCC	1338	1330	1328	1218	1308	1299
wagging $C(3)H_2$	1246	1250	1233	1131	1211	1214
bending HCC	1231	1226	1216	1114	1192	1195
rocking CH_2 + twisting CH_2	1101	1104	1091	1001	1072	1085
twisting CH_2	1054	1037	1028	942	1016	
wagging HCH	1002	983	971	884	951	935
stretching C−C	958	960	950	872	936	930
rocking CH_2	895	887	879	805	863	
stretching C−Br	737	726	704	642	692	698
twisting CH_2	579	563	530	480	519	543
bending CCC	404	400	388	354	377	391
bending CCBr	266	258	249	228	242	259
torsion $C-CH_2Br$	115	108	111	101	108	99
rotational constants						
A	0.645	0.642	0.642	0.638	0.639	
B	0.066	0.066	0.065	0.064	0.065	
C	0.064	0.064	0.063	0.062	0.063	
torsional barrier	3.3	3.2			3.2	

[a]Reference 23.

be seen, the three are endothermic processes, reaction (1) in ∼27 kcal mol^{-1}, reaction (2) in ∼60 kcal mol^{-1} and reaction (3) in ∼80 kcal mol^{-1}. Reaction (1) presents, along the minimum energy path, a maximum between the 3-bromopropene and the products HBr and allene. The transition state for this reaction was verified by following the IRC to both reactants and products (see Figure S1 in the Supporting Information). The computed values at 0 K, $\Delta H^{\#}_0$, are given in Table 3. A diagram of the profile of the potential energy surface for this reaction is shown in Figure 2. A standard normal-mode-analysis indicates that all transition-state structures obtained with the employed models lead to only one imaginary frequency indicating the presence of true transition states. The calculations predict four-center transition states (see Figure 1) with $\Delta H^{\#}_0$ values ranging from 56 to 63 kcal mol^{-1}. The geometrical parameters, rotational constants, and vibrational frequencies for this transition state are given in Tables 2 and S1 of Supporting Information. Channel (2) involves a barrierless simple bond fission process whose products, as Figure 2 shows, are located slightly below the electronic energy barrier of channel (1). Thus, channel (2) may be a possible reaction channel. Figure 3 shows the potential energy curve at different C−Br bond distances calculated with the remaining geometrical parameters fully optimized. As Table 3 shows, the computed activation enthalpy, $\Delta H^{\#}_0$, for channel (3) is ∼40 kcal mol^{-1} larger than the threshold enthalpies calculated for reactions (1) and (2), indicating that this process does not play any role in the decomposition reaction. In addition to these reactions, H_2 elimination processes from 3-bromopropene were analyzed. As Table S2 (Supporting Information) shows, all these pathways may certainly be ruled out on energetic grounds.

3.3. Theoretical Kinetic Analysis. In this section a kinetic analysis for channels (1) and (2) over a wide range of temperatures and pressures is presented. For simplicity, both reactions were studied in the high, in the low, and in the intermediate (falloff) pressure ranges independently. However, note that reactions (1) and (2) are probably, to some extension, coupled, and, therefore, a two-channel master−equation analysis appears necessary to quantify the errors inherent in the present approach.[35−39] The analysis of the intramolecular hydrogen abstraction pathway through a Br atom roaming to form HBr and $CH_2{=}C{=}CH_2$ as a process competitive to both (1) and (2) is beyond the scope of this work. However, this novel process has been demonstrated operative in similar systems.[40−43] Note, nevertheless, that one of the most reliable experimental studies of the 3-bromopropene decomposition[8] has provided conclusive evidence against dehydrobromination processes.

3.3.1. Limiting High-Pressure Rate Constants. Reaction $CH_2{=}CH{-}CH_2Br \rightarrow CH_2{=}C{=}CH_2 + HBr$. The limiting high-pressure rate constants for this reaction channel were calculated between 500 and 1400 K using the canonical formulation of the transition-state theory. The vibrational and rotational partition functions were evaluated using the molecular input data provided for the quantum-chemical calculations (Tables 1 and 2). The partition functions for the internal rotational motions of 3-bromopropene were calculated using the Troe's approach.[44] In this formalism, the partition function for a

DOI: 10.1021/acs.jpca.5b12581
J. Phys. Chem. A 2016, 120, 2285−2294

Table 2. Harmonic Vibrational Frequencies (in cm^{-1}), Approximate Assignments, and Rotational Constants (in cm^{-1}) for the Transition State of Channel (1) Calculated at Different Levels of Theory

	transition state channel (1)				
parameters	BMK	M06-2X	B3LYP	CBS-QB3	G4
vibrational frequencies					
stretching asym. CH_2	3261	3252	3242	2975	3206
stretching asym. CH_2	3252	3241	3235	2967	3197
stretching sym. CH_2	3147	3143	3140	2880	3103
stretching sym. CH_2	3145	3136	3134	2875	3097
stretching C−H	2444	2403	2494	2271	2469
stre asym CC	1647	1677	1634	1504	1618
bending HCH+stretch sym C−C	1535	1525	1524	1395	1496
bending CH_2 (both)	1448	1436	1442	1320	1415
bending CH_2 (both)	1267	1250	1267	1161	1241
bending HCC	1244	1229	1238	1133	1215
bending HCC	1086	1087	1064	973	1048
wagging CH_2	1055	1052	1038	943	1017
wagging CH_2	1005	1023	1001	913	982
wag+ rocking CH_2	992	970	989	907	980
wag+ rocking CH_2	964	952	951	869	930
twisting CH_2 (both)	526	523	541	495	530
twisting o C(2) oop	430	433	436	400	434
twisting CH_2	378	398	388	358	384
wagging CH_2	181	188	164	153	172
stretching C−Br	110	127	113	106	117
torsion CC (both)	363i	411i	270i	239i	273i
rotational constants					
A	0.372	0.376	0.368	0.367	0.368
B	0.052	0.054	0.051	0.051	0.052
C	0.046	0.048	0.045	0.045	0.046

Table 3. Reaction Enthalpies and Enthalpy Barriers at 0 K (in kcal mol^{-1}) for the 3-Bromopropene Dissociation Channels (1)−(3)

	CH_2=CH−CH_2Br → CH_2=C=CH_2 + HBr (1)			
	ΔH_r			
	isodesmic	direct		
level of theory	298 K	0 K	298 K	$\Delta H^{\#}_0$
M06-2X	25.7	24.1	25.5	63.8
CBS-QB3	28.0	27.7	28.9	57.1
G4	26.3	25.0	26.3	56.5
	CH_2=CH−CH_2Br → CH_2=CH−CH_2 + Br (2)			
	ΔH_r			
	isodesmic	direct		
level of theory	298 K	0 K	298 K	
M06-2X	55.2	56.7	57.5	
CBS-QB3	57.5	62.8	63.6	
G4	55.8	55.1	55.9	
	CH_2=CH−CH_2Br → CH_2=CH−CH + HBr (3)			
	ΔH_r	direct		
level of theory	0 K	298 K	$\Delta H^{\#}_0$	
M06-2X	76.2	77.5	95.2	
CBS-QB3	80.9	82.1	98.6	
G4	78.1	79.5	97.7	

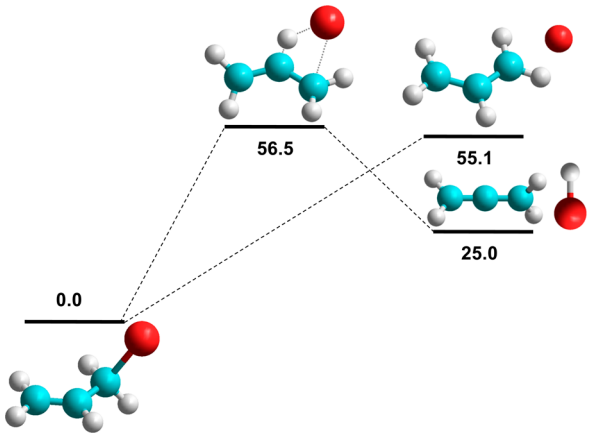

Figure 2. Schematic diagram of the potential energy surface (in kcal mol^{-1}) for the 3-bromopropene decomposition reaction calculated at the G4 level.

hindered rotor is obtained from interpolation between the free rotor and torsion partition functions. The CH_2Br moiety of the 3-bromopropene was considered as a hindered rotor with an estimated reduced moment of inertia of 24.6 amu $Å^2$ and a calculated barrier height of 3.2 kcal mol^{-1} (see Table 1 and Figure 4), which is in reasonable agreement with earlier reported values.[25] On the other hand, the transition state exhibits a rigid structure that avoids the internal rotation. The resulting high-pressure limit rate constants k_∞, pre-exponential factors A_∞, and activation energies $E_{a\infty}$ are listed in Table 4.

Over the studied temperature range a strict Arrhenius behavior for $k_{1,\infty}$ was observed. The plots for each level of theory are shown in Figure S2 of the Supporting Information. As can be seen, differences ranging from a factor of 13 to a factor of 1.6×10^3 where observed between the calculated DFT and composite ab initio $k_{1,\infty}$ values. The G4 is probably the

DOI: 10.1021/acs.jpca.5b12581
J. Phys. Chem. A 2016, 120, 2285−2294

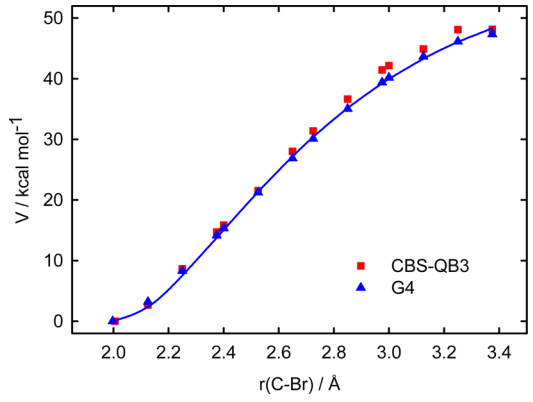

Figure 3. Potential energy curve for CH_2=CH−CH_2Br → CH_2=CH−CH_2 + Br calculated at different levels of theory. The solid line corresponds to a fit with a Morse potential; see Section 3.3.1.

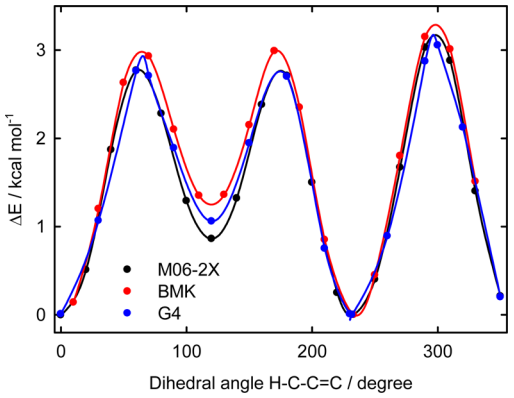

Figure 4. Potential energy barriers for internal rotation around C−C bond of 3-bromopropene calculated at different levels of theory.

more realistic model, and its results were employed for all kinetic analysis. The derived rate constants between 500 and 1400 K can be very well fitted with the expression

$$k_{1,\infty} = 2.1 \times 10^{13} \exp(-57.4 \text{ kcal mol}^{-1}/RT)\text{s}^{-1} \quad \text{(I)}$$

The comparison between the theoretical and the experimental data is shown in Figure 5. Clearly, the calculated rate constants $k_{1,\infty}$ differ significantly from those reported, suggesting that channel (1) appears not to be the predominant decomposition channel.

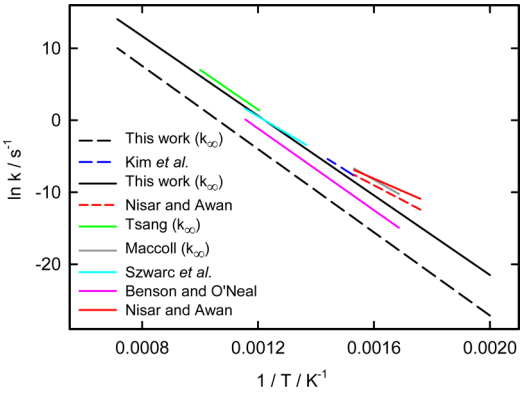

Figure 5. Temperature dependence of k_1 (dotted lines) and k_2 (solid line) (in s^{-1}).

Reaction CH_2=CH−CH_2Br → CH_2=CH−CH_2 + Br. As above-mentioned, reaction (2) involves a potential curve with a smooth transition between the reagent and the products (Figure 3). The kinetics of this barrierless reaction may be theoretically analyzed in terms of the statistical adiabatic channel model/classical trajectory (SACM/CT) treatment.[45] Unimolecular bond fission reactions and the reverse radical recombination reactions at the high-pressure limit are suitably described by this model. In particular, the recombination reaction CH_2=CH−CH_2 + Br → CH_2=CH−CH_2Br (−2) has been treated as the association between an atom and a linear rotor to form a nonlinear adduct.[45] For this, the molecular parameters and the energetics derived from the G4 calculations were employed. The high-pressure rate constants for a recombination process can be factorized as $k_{\text{rec},\infty} = f_{\text{rigid}} k^{\text{PST}}{}_{\text{rec},\infty}$, where $k^{\text{PST}}{}_{\text{rec},\infty}$ is the rate constant for phase space theory derived from the isotropic part of the potential, and f_{rigid} is the thermal rigidity factor that accounts for the potential anisotropy.[46] $k^{\text{PST}}{}_{\text{rec},\infty}$ can be calculated as

$$k^{\text{PST}}{}_{\text{rec},\infty} = f_e(8\pi kT/\mu)^{1/2}(-15.7706 - 8.6364X + 0.9975X^2)\beta^{-2} \quad \text{(II)}$$

Table 4. High-Pressure Rate Constants $k_{1,\infty}$ (in s^{-1}), Pre-Exponential Factors $A_{1,\infty}$ (in s^{-1}), Activation Energies $E_{a1,\infty}$ (in kcal mol^{-1}), and Electronic Energy Barriers $\Delta H^{\#}_{1,0}$ (in kcal mol^{-1}) for Reaction (1)

	$k_{1,\infty}$			
T	BMK	M06-2X	CBS-QB3	G4
500	2.70×10^{-15}	1.07×10^{-15}	9.16×10^{-13}	1.69×10^{-12}
600	1.24×10^{-10}	5.41×10^{-11}	1.50×10^{-8}	2.51×10^{-8}
700	2.69×10^{-7}	1.26×10^{-7}	1.55×10^{-5}	2.38×10^{-5}
800	8.59×10^{-5}	4.23×10^{-5}	2.85×10^{-3}	4.19×10^{-3}
900	7.68×10^{-3}	3.94×10^{-3}	1.64×10^{-1}	2.29×10^{-1}
1000	2.81×10^{-1}	1.48×10^{-1}	4.26×10^{0}	5.80×10^{0}
1100	5.36×10^{0}	2.92×10^{0}	6.10×10^{1}	7.97×10^{1}
1200	6.27×10^{1}	3.49×10^{1}	5.62×10^{2}	7.29×10^{2}
1400	3.02×10^{3}	1.74×10^{3}	1.86×10^{4}	2.33×10^{4}
$A_{1,\infty}$	3.09×10^{13}	2.18×10^{13}	2.07×10^{13}	2.09×10^{13}
$E_{a1,\infty}$	64.23	64.80	58.03	57.43
$\Delta H^{\#}_{1,0}$	63.12	63.79	57.14	56.53

DOI: 10.1021/acs.jpca.5b12581
J. Phys. Chem. A 2016, 120, 2285−2294

with $X = \ln(kT/D_e) - \beta r_{cm}$.[45] The expression (II) is based on a Morse potential $V = D_e[1 - \exp(-\beta(r - r_e)]^2$. For reaction (2) the bond dissociation energy D_e = 58.1 kcal mol^{-1} was calculated directly at the G4 level, and the range parameter β = 1.77 Å^{-1} was fitted (see Figure 3). For the equilibrium C−Br bond distance and the distance between the centers of mass of the two combining species the values r_e = 1.997 Å and r_{cm} = 2.9 Å were employed. A reduced mass of μ = 27.1 g mol^{-1} is calculated for the associating fragments, and f_e = 0.125 is the electronic degeneracy factor given by the ratio between the partition function of the adduct and the partition functions corresponding to the fragments. On the other hand, the rigidity factor was estimated as

$$f_{rigid} \approx 1 - 0.410 \exp[(X + 4)/2.359](1 + Z^2 + Z^8)^{-1/8} \quad \text{(III)}$$

where $Z = (C_{eff}/3 \text{ sen}^2 \gamma_e)^n/\gamma_1$. The parameter n is defined as $n = 1/(1 + 1.1/q + 1800/q^6) + 10/(20 + q^3)$ with $q = 3 \cos \gamma_e \approx 2$ and $\gamma_1 = (2^{1/2} - 3.3(q/2)^6 + (2^{1/2} + 7/q)\ (q/2)^8)/(1 + (q/2)^8\ q)$, being $\gamma_e = 40°$ the angle between the line connecting the centers of mass and the axes of the linear species. The anisotropy parameter is given by $C_{eff} = \varepsilon(r_e)^2/(2\ B\ D_e)\ (kT/D_e)^{2\alpha/\beta-1}\ [1 - 0.7\ (2\alpha/\beta - 1) + (2\alpha/\beta - 1)^2]$, where B = 0.3174 cm^{-1} is the rotational constant of the linear fragment obtained from the average of the two smallest rotational constants of the CH$_2$═CH−CH$_2$ radical (see Table S3 in the Supporting Information). The looseness parameter α accounts for the anisotropy of the potential along the reaction coordinate, and it is defined by the expression $\varepsilon_i(r) \approx \varepsilon(r_e) \exp[-\alpha\ (r - r_e)]$.[47] For the present reaction, the transitional mode quanta $\varepsilon(r_e)$ identified by following the corresponding r-dependence (Figure 6) were assigned to the vibrational frequencies of 242 and 377 cm^{-1} (see Table 1). The resulting individual α parameters are 0.55 and 0.86 Å^{-1}. The geometrical average values of $\varepsilon(r_e)$ = 302 cm^{-1} and α = 0.7 were used in the above C_{eff} expression. The resulting parameter ratio α/β = 0.40 is in reasonable agreement with the value derived by fitting a large number of experimental $k_{rec,\infty}$ values with a simplified SACM, α/β = 0.46 ± 0.09.[46]

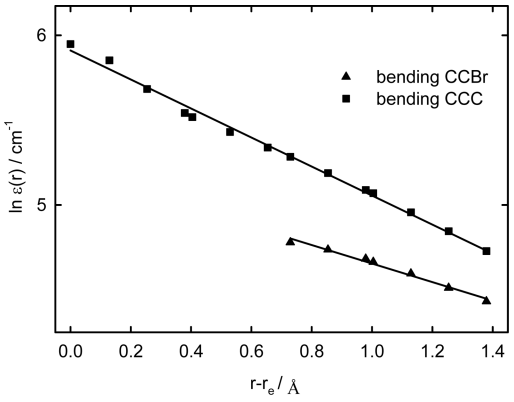

Figure 6. Dependence of the transitional modes of reaction (2) on the C−Br bond distance calculated at the G4 level. The derived α values are 0.55 and 0.86 Å^{-1}.

The values of $k^{PST}_{rec,\infty}$, f_{rigid}, and $k_{rec,\infty}$ calculated between 500 and 1400 K are listed in Table 5. High-pressure dissociation rate constants for reaction (2) were calculated using computed $k_{rec,\infty}$ values and estimated equilibrium constants K_c, $k_{2,\infty} = k_{rec,\infty}/K_c$ (Table 5). The K_c values were evaluated using the total partition functions of CH$_2$═CH−CH$_2$Br, CH$_2$═CH−CH$_2$, and Br. To this end, molecular parameters, harmonic vibrational frequencies, and reaction enthalpies at 0 K listed in Tables 1, 3, and S3 were employed. The internal rotations of the 3-bromopropene and the radical were considered as hindered motions, such that a vibrational frequency of 529 cm^{-1} for the torsional mode for CH$_2$CH−CH$_2$, and a reduced moment of inertia of 0.348 amu Å^2, were estimated. The corresponding torsional barriers are also included in Tables 1 and S3.

Over the studied temperature range a strict Arrhenius behavior for $k_{2,\infty}$ was observed, as Figure 5 shows. The fit to the calculated values is represented by eq IV.

$$k_{2,\infty} = 4.8 \times 10^{14} \exp(-55.0 \text{ kcal mol}^{-1}/RT)\text{s}^{-1} \quad \text{(IV)}$$

To study the dependence of $k_{2,\infty}$ with α, this parameter was varied from 0.5 to 0.9. Arrhenius parameters ranging from 3.9 × 10^{14} to 5.8 × 10^{14} s^{-1} and from 55.1 to 54.8 kcal mol^{-1} were obtained. Also, the results derived with the CBS-QB3 potential energy curve conduce to slightly larger $k_{2,\infty}$ values.

A comparison between the data listed in Tables 4 and 5 indicates that over the 500−1400 K range, $k_{2,\infty}$ is ca. 50 to 260 times larger than $k_{1,\infty}$. In addition, the computed $k_{2,\infty}$ are in better agreement with most of the previous results. This fact evidences channel (2) as dominant. In fact, our data for channel (2) are in good concordance with the results of Tsang[8] and Szwarc et al.[6] and agree reasonably with those derived by Maccoll[5] and with the Benson's recommended rate constants for reaction (2).[7] On the other hand, the studies of Kim[9] and Nisar and Awan[10] conduce to rate constants for channel (1) ~2 orders of magnitude higher than those obtained in the present investigation for that channel. Also in ref 10, rate constants for the global reaction were determined. The obtained results indicate that reaction (2) is the main channel.

In addition, the rate constant for the recombination reaction (−2) obtained in the present work can be written as a function of temperature as

Table 5. Recombination Rate Constants $k^{PST}_{rec,\infty}$ and $k_{rec,\infty}$ (in cm^3 molecule^{-1} s^{-1}) and Thermal Rigidity Factors f_{rigid} for Reaction (−2), Equilibrium Constants K_c (in cm^3 Molecule^{-1}) and Dissociation Rate Constants $k_{2,\infty}$ (in s^{-1}) for Reaction (2). All Derived at the G4 Level

T	$k^{PST}_{rec,\infty}$	f_{rigid}	$k_{rec,\infty}$	K_c	$k_{2,\infty}$
500	1.16 × 10^{-10}	0.579	6.74 × 10^{-11}	1.52 × 10^{-1}	4.44 × 10^{-10}
600	1.23 × 10^{-10}	0.584	7.20 × 10^{-11}	1.55 × 10^{-5}	4.65 × 10^{-6}
800	1.35 × 10^{-10}	0.593	7.99 × 10^{-11}	1.66 × 10^{-10}	5.00 × 10^{-1}
1000	1.44 × 10^{-10}	0.600	8.66 × 10^{-11}	1.81 × 10^{-13}	4.78 × 10^{2}
1200	1.53 × 10^{-10}	0.605	9.23 × 10^{-11}	1.98 × 10^{-15}	4.66 × 10^{4}
1400	1.60 × 10^{-10}	0.608	9.70 × 10^{-11}	8.04 × 10^{-17}	1.21 × 10^{6}

DOI: 10.1021/acs.jpca.5b12581
J. Phys. Chem. A 2016, 120, 2285−2294

Table 6. Contributing Factors to k_0^{SC} and the Resulting k_0 Values for Reaction (1) for M = 3-Bromopropene ($-\langle\Delta E\rangle \approx 477$ cm^{-1})

parameters	500 K	600 K	643 K	800 K	1000 K	1400 K
Z_{LJ}[a]	5.00×10^{-10}	5.20×10^{-10}	5.26×10^{-10}	5.53×10^{-10}	5.84×10^{-10}	6.38×10^{-10}
F_E	1.26	1.33	1.36	1.48	1.68	2.23
F_{rot}	3.20	2.84	2.71	2.33	1.98	1.53
F_{rotint}	4.28	3.42	3.14	2.40	1.84	1.25
Q_{vib}	7.07	1.43×10^{1}	1.95×10^{1}	6.22×10^{1}	2.73×10^{2}	4.60×10^{3}
$k_{1,0}^{SC}/[M]$[a]	1.2×10^{-24}	7.4×10^{-21}	1.3×10^{-19}	2.2×10^{-16}	5.9×10^{-14}	1.3×10^{-11}
$k_{1,0}/[M]$[a]	4.9×10^{-25}	2.9×10^{-21}	5.0×10^{-20}	6.5×10^{-17}	1.8×10^{-14}	2.5×10^{-12}

[a] In cm^3 molecule^{-1} s^{-1}.

Table 7. Contributing Factors to k_0^{SC} and the Resulting k_0 Values for Reaction (2) for M = 3-Bromopropene ($-\langle\Delta E\rangle \approx 477$ cm^{-1})

parameters	500 K	600 K	643 K	800 K	1000 K	1400 K
Z_{LJ}[a]	5.00×10^{-10}	5.20×10^{-10}	5.26×10^{-10}	5.53×10^{-10}	5.84×10^{-10}	6.38×10^{-10}
F_E	1.26	1.33	1.37	1.49	1.69	2.27
F_{rot}	6.63	5.30	4.87	3.71	2.80	1.82
F_{rotint}	4.18	3.33	3.06	2.34	1.79	1.22
Q_{vib}	7.07	1.43×10^{1}	1.95×10^{1}	6.22×10^{1}	2.73×10^{2}	4.60×10^{3}
$k_{2,0}^{SC}/[M]$[a]	7.5×10^{-24}	3.2×10^{-20}	4.9×10^{-19}	6.0×10^{-16}	1.2×10^{-13}	1.8×10^{-11}
$k_{2,0}/[M]$[a]	3.0×10^{-24}	1.3×10^{-20}	2.0×10^{-19}	1.8×10^{-16}	3.6×10^{-14}	3.6×10^{-12}

[a] In cm^3 molecule^{-1} s^{-1}.

$$k_{rec,\infty} = 9.0 \times 10^{-11}(T/1000)^{0.34} \quad \text{(V)}$$

An experimental study of reaction (−2) at 298 K and 1 Torr of He yields a value of $(2.0 \pm 0.5) \times 10^{-10}$ cm^3 molecule^{-1} s^{-1}.[48] According to our analysis of the falloff region in Section 3.3.3 (Figure S4), the bimolecular rate constant determined in ref 48 corresponds to its high-pressure limit value, and it may be compared with the value of 5.9×10^{-11} cm^3 molecule^{-1} s^{-1} derived from (V) at 298 K. Both values are consistent if the error in the experimental determination of ref 48 is taken into account and we bear in mind that our estimation has a mean error of approximately a factor of 2.

3.3.2. Limiting Low-Pressure Rate Coefficients. To compare more precisely the theoretical results with previous investigations, the pressure dependence of reactions (1) and (2) was studied. To this end, limiting low-pressure rate constants were calculated. The falloff behavior of the dissociation channels (1) and (2) is analyzed in the next section. At the low-pressure limit, the rate coefficient k_0 can be represented by the product of the collision efficiency β_c and the strong-collision rate constant k_0^{SC}.[44] Troe's factorized formalism[44] was applied to calculate k_0^{SC}, which is described by specific independent factors for a given bath gas M such as

$$k_0^{SC} = [M]Z_{LJ}(\rho_{vib,h}(E_0)kT/Q_{vib})\exp(-E_0/kT)F_{anh}F_E F_{rot} F_{rotint} \quad \text{(VI)}$$

These factors were calculated employing the molecular parameters listed in Tables 1, 2, and S3. Both the harmonic vibrational density of states $\rho_{vib,h}(E_0)$ (at the threshold dissociation energy $E_0 \approx \Delta H^{\ddagger}_0$) and the anharmonicity factor F_{anh} of the decomposed molecule are temperature-independent. The respective values for the 3-bromopropene decomposition through reactions (1) and (2) are 4.65×10^9 (kcal mol^{-1})$^{-1}$ (E_0 = 56.5 kcal mol^{-1}) and 3.43×10^9 (kcal mol^{-1})$^{-1}$ (E_0 = 55.1 kcal mol^{-1}) and 1.11 and 1.08. The other factors account for the spread of internal energies F_E, external rotations F_{rot}, and internal rotations F_{rotint}. In addition, Z_{LJ} is the Lennard-Jones collision frequency, and Q_{vib} is the vibrational partition function of 3-bromopropene. In the F_{rot} calculation for reaction (1) the molecular properties of the above-described tight transition state were employed, while the barrierless potential of Figure 3 was employed for reaction (2). The torsional barrier given in Table 1 was employed for the F_{rotint} calculations. To evaluate Z_{LJ}, Lennard-Jones parameters σ and ε/k of 5.3 Å and 415.8 K, respectively, were estimated for 3-bromopropene from molecular critical properties.[33] The obtained strong collision low-pressure rate coefficients k_0^{SC} were corrected by weak collision effects using a reasonable β_c value of 0.4 for M = 3-bromopropene at 500 K. Employing the simple expression that connects β_c with the average energy transferred in activating and deactivating collisions: $-\langle\Delta E\rangle \approx F_E\, kT\, \beta_c/(1-\beta_c^{1/2})$,[44] we roughly estimate $-\langle\Delta E\rangle \approx 477$ cm^{-1}. Assuming a temperature-independent $\langle\Delta E\rangle$, β_c values of 0.4 at 600 and 643 K, 0.3 at 800 and 1000 K, and 0.2 at 1400 K were estimated. The resulting k_0 (with a mean error of about a factor of 2[44,49]) are shown in Tables 6 and 7 and can be expressed as

$$k_{1,0} = [M]1.3 \times 10^{-3}(T/1000)^{0.71} \times \exp(56.5 \text{ kcal mol}^{-1}/RT) \text{ cm}^3 \text{ molecule}^{-1} \text{ s}^{-1} \quad \text{(VII)}$$

$$k_{2,0} = [M]1.9 \times 10^{-3}(T/1000)^{-0.82} \times \exp(55.1 \text{ kcal mol}^{-1}/RT) \text{ cm}^3 \text{ molecule}^{-1} \text{ s}^{-1} \quad \text{(VIII)}$$

It can be seen from Tables 6 and 7 that the differences between $k_{2,0}$ and $k_{1,0}$ are much smaller than those observed for the high-pressure rate constants.

3.3.3. Falloff Region. The derived limiting rate constants allow to characterize the decomposition channels of 3-bromopropene over a wide pressure range. The analysis was performed using the Troe's reduced formalism[49]

$$k/k_\infty = F^{LH}(x)F(x) \quad \text{(IX)}$$

DOI: 10.1021/acs.jpca.5b12581
J. Phys. Chem. A 2016, 120, 2285−2294

Here $x = k_0/k_\infty$, while $F^{LH}(x) = x/(1 + x)$ results of the simple Lindemann−Hinshelwood mechanism, and $F(x)$, the broadening factor, accounts for corrections due to the energy and total angular momentum dependence of the excited species and for the multistep character of the collisional energy transfer. At high temperatures[50] and when the center broadening factor $F_{cent} = F(x = 1)$ is smaller to ∼0.4 (as the present 0.19−0.31), $F(x)$ is represented by $F(x) = (1+ x/x_0)/[1 + (x/x_0)^n]^{1/n}$ with $n = [\ln 2/\ln(2/F_{cent})][1 - b + b(x/x_0)^q]$ where $q = (F_{cent} - 1)/\ln(F_{cent}/10)$, $x_0 = 1$, and $b = 0.2$.[51] F_{cent} is approximated as $F^{SC}_{cent} F^{WC}_{cent}$, where F^{SC}_{cent} is the strong collision broadening factor[52] and $F^{WC}_{cent} \approx \beta_c^{0.14}$ is the weak collision broadening factor.[50] For M = 3-bromopropene a $\beta_c = 0.4$ was employed at 600 and 643 K; for M = toluene a $\beta_c = 0.3$ was estimated at 800 K, assuming a value of $-\langle\Delta E\rangle \approx 500$ cm^{-1}.[53] A reasonable value of $\beta_c = 0.1$ was employed for M = Ar at 600 and 1000 K. Effective Lennard-Jones parameters of $\sigma = (\sigma_{3\text{-bromopropene}} + \sigma_M)/2$ and $\varepsilon/k = (\varepsilon_{3\text{-bromopropene}}/k\ \varepsilon_M/k)^{1/2}$ were employed for the experiments performed in the presence of M = Ar (σ_{Ar} = 3.465 Å and ε_{Ar}/k = 113.5 K) and M = toluene ($\sigma_{toluene}$= 5.923 Å and $\varepsilon_{toluene}/k$ = 407.8 K),[54] respectively. To calculate F_{cent} for channel (1) the barrier energy $E_0 \approx \Delta H^{\ddagger}_0$ = 56.5 kcal mol^{-1}, and the vibrational frequencies for the transition state were used. For channel (2) the threshold energy $E_0 \approx$ 55.1 kcal mol^{-1}, and the vibrational frequencies for the 3-bromopropene were employed.

The falloff curves obtained for both channels at the temperatures of the available experimental data are depicted in Figure 7. Plots for the individual channels in a normalized form at 500−1400 K are included in the Supporting Information (Figures S3 and S4). As can be observed from Figure 7, falloff curves for both channels are more separated at high pressures. At higher temperatures, the separation between the curves for both channels is smaller compared to the results at lower temperatures. This could be attributed to the differences in F_{rot} and $\rho_{vib,h}(E_0)$ values for each channel. With the exception of the results from Kim et al.[9] (corresponding to channel (1)) and Nisar and Awan,[10] the rest of the experimental values compare reasonably well with our predictions for channel (2), pointing out this channel as the dominant decomposition fate for 3-bromopropene. In fact, the present rate constants are a factor of ∼2 smaller than those reported by Szwarc et al.[6] and Tsang.[8] Conversely, our calculations underestimate by factors close to 12 and 30 the results of Maccoll[5] and Nisar and Awan,[10] respectively. Some time ago, Benson and O'Neal[7] suggested that the static experiments of Maccoll[5] could be perturbed by a chain component. This fact might explain the discrepancy with our results. On the other hand, regarding the results of Nisar and Awan,[10] similar or even larger differences between calculated and experimental rate constants have been found in the thermal decompositions of 2-chloropropene (factor of ∼20)[11,55] and 2-bromopropene (factor of ∼6000).[12,56] However, in both cases the theoretical data agree very well with those determined in more direct shock waves studies.[57] The reason for the above-mentioned pronounced discrepancies remains still unclear.

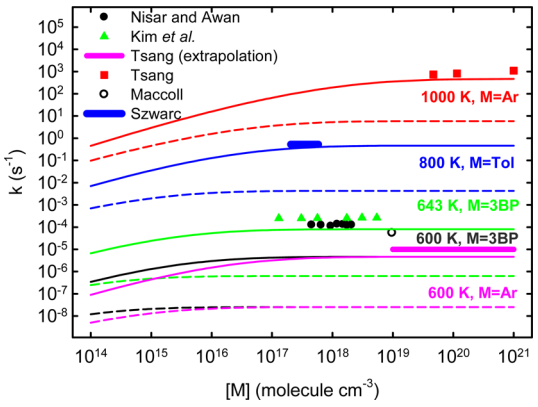

Figure 7. Falloff curves for reactions (1) (dotted lines) and (2) (solid line). 3BP = 3-bromopropene; Tol = toluene.

Finally, the branching ratio for the thermal decomposition of 3-bromopropene through reaction channel (2) was estimated as $\varphi = k_2/(k_1 + k_2)$. At the low-pressure limit, values for φ of 0.86, 0.67, and 0.59 were derived at 500, 1000, and 1400 K, respectively. For the same temperatures, φ values of 0.996, 0.988, and 0.982 were calculated at the high-pressure limit.

4. CONCLUSIONS

The present quantum-mechanical and kinetic study of the gas-phase thermal decomposition of 3-bromopropene over extended temperature and pressure ranges allows to elucidate contradictory and incomplete kinetic information for this reaction. The results indicate that the dominant reaction channel is the breaking of the C−Br bond in CH_2═CH−CH_2Br leading to the formation of Br and the CH_2═CH−CH_2 radical. Besides, the falloff analysis shows that all reported experimental studies are very close to the high-pressure limit. The rate constant for the primary dissociation is $k_\infty = 4.8 \times 10^{14}$ exp(−55.0 kcal mol^{-1}/RT) s^{-1} in the range of 500−1400 K, ∼50−260 times higher than the values estimated for the channel CH_2═CH−CH_2Br → CH_2═C═CH_2 + HBr. The calculated rate constants are in good agreement with those reported by Maccoll,[5] Szwarc et al.,[6] Benson and O'Neal[7] and Tsang,[8] but they differ from the results of Kim et al.[9] and Nisar and Awan.[10] However, it appears interesting to mention that a coupled kinetic analysis of reactions (1) and (2) in terms of a two-channel master-equation analysis should be of considerable interest to test our estimations. In addition, a standard enthalpy of formation for the 3-bromopropene at 298 K of 10.6 ± 1.5 kcal mol^{-1} was estimated.

■ ASSOCIATED CONTENT

Supporting Information

The Supporting Information is available free of charge on the ACS Publications website at DOI: 10.1021/acs.jpca.5b12581.

Structural parameters for 3-bromopropene and its transition state. Reaction and activation enthalpies for the 3-bromopropene decomposition channels. Harmonic vibrational frequencies, rotational constants, and torsional barrier for the CH_2═CH−CH_2 radical. Relative energy along the intrinsic reaction coordinate for channel (1). Temperature dependence of $k_{1,\infty}$ at different levels of theory. Reduced falloff curves for channels (1) and (2). (PDF)

■ AUTHOR INFORMATION

Corresponding Author

*Phone: +54-221-4257430. Fax: +54-221-4254642. E-mail: mtucceri@inifta.unlp.edu.ar.

Notes

The authors declare no competing financial interest.

DOI: 10.1021/acs.jpca.5b12581
J. Phys. Chem. A 2016, 120, 2285−2294

■ ACKNOWLEDGMENTS

This research project was supported by the Universidad Nacional de La Plata (11/X676), the Consejo Nacional de Investigaciones Científicas y Técnicas CONICET (PIP-615, PIP-1134), and the Agencia Nacional de Promoción Científica y Tecnológica (PICT-478).

■ REFERENCES

(1) *Reactive Halogen Compounds in the Atmosphere, The Handbook of Environmental Chemistry;* Fabian, P., Singh, O. N., Eds.; Springer-Verlag: Berlin, Germany, 1999; Vol. *4*.

(2) Kerkweg, A.; Jockel, P.; Warwick, N.; Gebhardt, S.; Brenninkmeijer, C. A. M.; Lelieveld, J. Consistent Simulation of Bromine Chemistry from the Marine Boundary Layer to the Stratosphere – Part 2: Bromocarbons. *Atmos. Chem. Phys.* **2008**, *8*, 5919–5939.

(3) Raimund, S.; Quack, B.; Bozec, Y.; Vernet, M.; Rossi, V.; Garçon, V.; Morel, Y.; Morin, P. Sources of Short-Lived Bromocarbons in the Iberian Upwelling System. *Biogeosciences* **2011**, *8*, 1551–1564.

(4) Hossaini, R.; Mantle, H.; Chipperfield, M. P.; Montzka, S. A.; Hamer, P.; Ziska, F.; Quack, B.; Krüger, K.; Tegtmeier, S.; Atlas, E.; et al. Evaluating Global Emission Inventories of Biogenic Bromocarbons. *Atmos. Chem. Phys.* **2013**, *13*, 11819–11838.

(5) Maccoll, A. The Kinetics of the Pyrolysis of Allyl Bromide. *J. Chem. Phys.* **1949**, *17*, 1350–1351.

(6) Szwarc, M.; Ghosh, B. N.; Sehon, A. H. The C–Br Bond Dissociation Energy in Benzyl Bromide and Allyl Bromide. *J. Chem. Phys.* **1950**, *18*, 1142–1149.

(7) Benson, S. W.; O'Neal, H. E. *Kinetic data on Gas Phase Unimolecular Reactions;* National Standard Reference Data Series, No. 21; National Bureau of Standards, 1970.

(8) Tsang, W. Single-Pulse Shock-Tube Studies on the Decomposition of 1,2-Dibromoperfluoroethane and Allyl Bromide. *J. Phys. Chem.* **1984**, *88*, 2812–2817.

(9) Kim, S. H.; Choo, K. Y.; Jung, K.-H. A Gas Phase Kinetic Study on the Thermal Decomposition of $ClCH_2CH_2CH_2Br$. *Bull. Korean Chem. Soc.* **1989**, *10*, 262–269.

(10) Nisar, J.; Awan, I. A. Kinetics of the Gas_Phase Thermal Decomposition of 3-Bromopropene. *Kinet. Catal.* **2011**, *52*, 487–492.

(11) Tucceri, M. E.; Badenes, M. P.; Cobos, C. J. Quantum Chemical and Kinetics Study of the Thermal Gas Phase Decomposition of 2-Chloropropene. *J. Phys. Chem. A* **2013**, *117*, 10218–10227.

(12) Bracco, L. L. B.; Badenes, M. P.; Tucceri, M. E.; Cobos, C. J. Theoretical kinetic study of the unimolecular decomposition of 2-bromopropene. *Chem. Phys. Lett.* **2014**, *608*, 386–392.

(13) Frisch, M. J.; Trucks, G. W.; Schlegel, H. B.; Scuseria, G. E.; Robb, M. A.; Cheeseman, J. R.; Scalmani, G.; Barone, V.; Mennucci, B.; Petersson, G. A. et al. *Gaussian 09,* revision A.02; Gaussian, Inc: Wallingford, CT, 2009.

(14) Becke, A. D. Density Functional Thermochemistry. III. The Role of Exact Exchange. *J. Chem. Phys.* **1993**, *98*, 5648–5652.

(15) Becke, A. D. Density-Functional Exchange-Energy Approximation with Correct Asymptotic Behaviour. *Phys. Rev. A: At., Mol., Opt. Phys.* **1988**, *38*, 3098–3100.

(16) Lee, C.; Yang, W.; Parr, R. G. Development of the Colle-Salvetti Correlation-Energy Formula into a Functional of the Electron Density. *Phys. Rev. B: Condens. Matter Mater. Phys.* **1988**, *37*, 785–789.

(17) Boese, A. D.; Martin, J. M. L. Development of Density Functionals for Thermochemical Kinetics. *J. Chem. Phys.* **2004**, *121*, 3405–3416.

(18) Zhao, Y.; Truhlar, D. G. The M06 Suite of Density Functionals for Main Group Thermochemistry, Thermochemical Kinetics, Noncovalent Interactions, Excited States, and Transition Elements: Two New Functionals and Systematic Testing of Four M06-Class Functionals and 12 Other Functionals. *Theor. Chem. Acc.* **2008**, *120*, 215–241.

(19) Montgomery, J. A., Jr.; Frisch, M. J.; Ochterski, J. W.; Petersson, G. A. A Complete Basis Set Model Chemistry. VI. Use of Density Functional Geometries and Frequencies. *J. Chem. Phys.* **1999**, *110*, 2822–2827.

(20) Montgomery, J. A., Jr.; Frisch, M. J.; Ochterski, J. W.; Petersson, G. A. A Complete Basis Set Model Chemistry. VII. Use of The Minimum Population Localization Method. *J. Chem. Phys.* **2000**, *112*, 6532–6542.

(21) Curtiss, L. A.; Redfern, P. C.; Raghavachari, K. Gaussian-4 Theory. *J. Chem. Phys.* **2007**, *126*, 084108.

(22) Niide, Y.; Takano, M.; Satoh, T.; Sasada, Y. Microwave Spectrum, Molecular Structure, and Nuclear Quadrupole Coupling Constants of 3-Bromopropene. *J. Mol. Spectrosc.* **1976**, *63*, 108–119.

(23) Durig, J. R.; Jalilian, M. R. Conformational Analysis of Gaseous 3-bromopropene from Low-Frequency Raman Data. *J. Phys. Chem.* **1980**, *84*, 3543–3547.

(24) Schei, E.; Shen, Q. The Molecular Structure and Conformational Composition of 3-Bromopropene as Determined by Gas-Phase Electron Diffraction. *J. Mol. Struct.* **1982**, *81*, 269–276.

(25) Kolandaivel, P.; Jayakumar, N. Structure and Conformational Stability of CH_2CHCH_2X (X. F, Cl and Br) Molecules – Post Hartree – Fock and Density Functional Theory Methods. *J. Mol. Struct.: THEOCHEM* **2000**, *507*, 197–206.

(26) Hehre, W. J.; Radom, L.; Schleyer, P. v. R.; Pople, J. A. *Ab Initio Molecular Orbital Theory;* Wiley: New York, 1986.

(27) Ruscic, B. Active Thernochemical Tables (ATcT) values based on ver. 1.112 of the Thermochemical Network, 2013; http://ATcT.anl.gov.

(28) Chase, M. W., Jr. NIST-JANAF Thermochemical Tables, 4th ed.; *J. Phys. Chem. Ref. Data*, **1998**, Monograph No. 9.

(29) Ochterski, J. W. Thermochemistry in Gaussian. http://www.gaussian.com/g_whitepap/thermo.htm.

(30) Trager, J. C. A Study of the Allyl Cation Thermochemistry by Photoionization Mass Spectrometry. *Int. J. Mass Spectrom. Ion Processes* **1984**, *58*, 259–271.

(31) Cox, J. D.; Pilcher, G. *Thermochemistry of Organic and Organometallic Compounds;* Academic Press: New York, 1970.

(32) Gellner, O. H.; Skinner, H. A. Dissociation Energies of Carbon–Halogen Bonds. The Bond Strengths Allyl–X and Benzyl–X. *J. Chem. Soc.* **1949**, *0*, 1145–1148.

(33) NIST Chemistry WebBook. NIST Standard Reference Database Number 69, http://webbook.nist.gov/chemistry.

(34) Sander, S. P.; Friedl, R. R.; Barker, J. R.; Golden, D. M.; Kurylo, M. J.; Wine, P. H.; Abbatt, J. P. D.; Burkholder, J. B.; Kolb, C. E.; Moortgat, G. K.; Huie, R. E.; Orkin, V. L. *Chemical Kinetics and Photochemical Data for Use in Atmospheric Studies;* NASA/JPL Data Evaluation, JPL Publication 06–2 Evaluation No. 17, NASA: Pasadena, CA, June 1, 2011; http://jpldataeval.jpl.nasa.gov/.

(35) Miller, J. A. Master Equation Methods in Gas Phase Chemical Kinetics. *J. Phys. Chem. A* **2006**, *110*, 10528–10544.

(36) Miller, J. A.; Klippenstein, S. J. Determining Phenomenological Rate Coefficients From a Time-Dependent, Multiple-Well Master Equation: "Species Reduction" at High Temperatures. *Phys. Chem. Chem. Phys.* **2013**, *15*, 4744–4753.

(37) Robertson, S. H.; Pilling, M. J.; Jitariu, L. C.; Hillier, I. H. Master Equation Methods for Multiple Well Systems: Application to the 1-,2-pentyl system. *Phys. Chem. Chem. Phys.* **2007**, *9*, 4085–4097.

(38) Glowacki, D. R.; Liang, C.-H.; Morley, C.; Pilling, M. J.; Robertson, S. H. MESMER: an Open-Source Master Equation Solver for Multi-Energy Well Reactions. *J. Phys. Chem. A* **2012**, *116*, 9545–9560.

(39) Barker, J. R. Multiple-Well, Multiple-Path Unimolecular Reaction Systems. I. MultiWell Computer Program Suite. *Int. J. Chem. Kinet.* **2001**, *33*, 232–245.

(40) Townsend, D.; Lahankar, S. A.; Lee, S. K.; Chambreau, S. D.; Suits, A. G.; Zhang, X.; Rheinecker, J.; Harding, L. B.; Bowman, J. M. The Roaming Atom: Straying from the Reaction Path in Formaldehyde Decomposition. *Science* **2004**, *306*, 1158–1161.

(41) Zhang, X.; Rheinecker, J. L.; Bowman, J. M. Quasiclassical Trajectory Study of Formaldehyde Unimolecular Dissociation: H2CO \H2+CO, H+HCO. *J. Chem. Phys.* **2005**, *122*, 114313–1142138.

DOI: 10.1021/acs.jpca.5b12581
J. Phys. Chem. A 2016, 120, 2285–2294

(42) Sivaramakrishnan, R.; Michael, J. V.; Klippenstein, S. J. Direct Observation of Roaming Radicals in the Thermal Decomposition of Acetaldehyde. *J. Phys. Chem. A* **2010**, *114*, 755−764.
(43) Harding, L. B.; Georgievskii, Y.; Klippenstein, S. J. Roaming Radical Kinetics in the Decomposition of Acetaldehyde. *J. Phys. Chem. A* **2010**, *114*, 765−777.
(44) Troe, J. Theory of Thermal Unimolecular Reactions at Low Pressures. II. Strong Collision Rate Constants. Applications. *J. Chem. Phys.* **1977**, *66*, 4758−4775.
(45) Maergoiz, A. I.; Nikitin, E. E.; Troe, J.; Ushakov, V. G. Classical trajectory and Statistical Adiabatic Channel Study of the Dynamics of Capture and Unimolecular Bond Fission. IV. Valence Interactions Between Atoms and Linear Rotors. *J. Chem. Phys.* **1998**, *108*, 5265−5280.
(46) Cobos, C. J.; Troe, J. Theory of Thermal Unimolecular Reactions at High Pressures. II. Analysis of Experimental Results. *J. Chem. Phys.* **1985**, *83*, 1010−1015.
(47) Quack, M.; Troe, J. Specific Rate Constants of Unimolecular Processes. *Ber. Bunsenges. Phys.Chem.* **1974**, *78*, 240−252.
(48) Bedjanian, Y.; Poulet, G.; Le Bras, G. Low-Pressure Study of the Reactions of Br Atoms with Alkenes. 1. Reaction with Propene. *J. Phys. Chem. A* **1998**, *102*, 5867−5875.
(49) Troe, J. Predictive Possibilities of Unimolecular Rate Theory. *J. Phys. Chem.* **1979**, *83*, 114−126.
(50) Gilbert, R. G.; Luther, K.; Troe, J. Theory of Thermal Unimolecular Reactions in the Fall-Off Range. II. Weak Collision Rate Constants. *Ber. Bunsenges. Phys. Chem.* **1983**, *87*, 169−177.
(51) Troe, J.; Ushakov, V. G. Representation of "Broad" Falloff Curves for Dissociation and Recombination Reactions. *Z. Phys. Chem.* **2014**, *1*, 1−10.
(52) Troe, J. Theory of Thermal Unimolecular Reactions in the Fall-Off Range. I. Strong Collision Rate Constants. *Ber. Bunsenges. Phys. Chem.* **1983**, *87*, 161−169.
(53) Heymann, M.; Hippler, H.; Troe, J. Collisional Deactivation of Vibrationally Highly Excited Polyatomic Molecules. IV. Temperature Dependence of $< \Delta E >$. *J. Chem. Phys.* **1984**, *80*, 1853−1860.
(54) Mourits, F. M.; Rummens, F. H. A. A Critical Evaluation of Lennard-Jones and Stockmayer Potential Parameters and of Some Correlation Methods. *Can. J. Chem.* **1977**, *55*, 3007−3020.
(55) Nisar, J.; Awan, I. A. A Gas-Phase Kinetic Study on the Thermal Decomposition of 2-Chloropropene. *Kinet. Catal.* **2008**, *49*, 461−465.
(56) Nisar, J.; Awan, I. A. Kinetics of Thermal Gas-Phase Decomposition of 2-Bromopropene Using Static System. *Int. J. Chem. Kinet.* **2007**, *39*, 1−5.
(57) Roy, K.; Awan, I. A.; Manion, J. A.; Tsang, W. Thermal Decomposition of 2-Bromopropene and 2-Chloropropene. *Phys. Chem. Chem. Phys.* **2003**, *5*, 1806−1810.

DOI: 10.1021/acs.jpca.5b12581
J. Phys. Chem. A 2016, 120, 2285−2294